



HAL
open science

Observer-Based Flux Controller for Synchronous Reluctance Motor Including Magnetic Saturation

Romain Delpoux, Zohra Kader, Thomas Huguet

► **To cite this version:**

Romain Delpoux, Zohra Kader, Thomas Huguet. Observer-Based Flux Controller for Synchronous Reluctance Motor Including Magnetic Saturation. *Electrimacs*, May 2024, Castelló de la Plana, Spain. hal-04583789v1

HAL Id: hal-04583789

<https://hal.science/hal-04583789v1>

Submitted on 22 May 2024 (v1), last revised 23 May 2024 (v2)

HAL is a multi-disciplinary open access archive for the deposit and dissemination of scientific research documents, whether they are published or not. The documents may come from teaching and research institutions in France or abroad, or from public or private research centers.

L'archive ouverte pluridisciplinaire **HAL**, est destinée au dépôt et à la diffusion de documents scientifiques de niveau recherche, publiés ou non, émanant des établissements d'enseignement et de recherche français ou étrangers, des laboratoires publics ou privés.

Observer-Based Flux Controller for Synchronous Reluctance Motor Including Magnetic Saturation

Romain Delpoux · Zohra Kader · Thomas Huguet

Abstract The present article focuses on the observation of flux for Synchronous Reluctance Motor (SynRM) in the presence of magnetic saturation and cross-saturation. In this context, the proposed observer is able to provide flux estimation based on the measured current only. The designed observer makes it possible to propose a flux-based control which, in presence of saturation, is simpler to implement than a classic current-based control. Simulation results, with a model obtained from Finite Element Analysis (FEA) using Finite Element Method Magnetics (FEMM), show the performance of the proposed approach.

1 Introduction

Permanent Magnet Synchronous Motors (PMSM), using rare-earth, are considered as the main candidate in most industrial applications due to their high performance. While these machines notably make it possible to offer vehicles that do not emit exhaust fumes and therefore reduce CO₂ emissions, environmental impacts of rare earth materials and supply risks, e.g. restricted access and price volatility, impacts their cost [11, 15]. The development of applications using rare-earth-free motors is today a strategic priority. In this context, Synchronous Reluctance Motor (SynRM) technology gains more and more interest since a few years and becomes a serious competitor [8, 10]. Due to technical advances in computer science, electronics and power electronics, these

machines compete with asynchronous machines in terms of efficiency. New designs also continually improve them [3], these machines are now tending to compete with the PMSM [6] in various industrial applications [2, 9], due to increased efficiency and reduced weight [16].

Under rated condition magnetic flux saturation occurs heavily, causing large nonlinearities [10]. Maximum Torque Per Ampere (MTPA) control is important to optimize energy efficiency of the motor. Recently, MTPA control for SynRM and interior permanent magnet motor drives has received a lot of attention as the recent literature review [17] can attest. In this article it is clearly stated that the presence of magnetic nonlinearities such as saturation and cross saturation makes the use of the notion of inductance complex, due to the difficulties about the precise knowledge of the differential inductances which intervene. Since inductances are nonlinear, it seems interesting to focus on the flux rather than on current and thus to get rid of the problems of differential inductances. While flux is difficult to measure, it is often obtained from Look Up Table (LUT) as function of current [7]. To avoid these LUT flux observation for these nonlinear machines are a good prospect. In recent years, flux observers for machines in which saturations are negligible thanks to the presence of magnets were introduced in the literature [4, 13]. The importance of observer-based flux control for SynRM has been highlighted in [1] but here again, saturations are not considered. In more recent work [18], magnetic saturation is considered.

As the SynRM parameters are likely to vary over time, this paper presents a novel observer capable of estimating the flux based on the current measurements only, while the current-flux mapping is nonlinear. The proposed observer is designed with the assumption that flux in the motor can be approximated by a linear function of the currents and a slowly variable parameters to be estimated. It allows proposing a flux-based control strategy which, in the presence of

R. Delpoux
INSA Lyon, Université Claude Bernard Lyon 1, Ecole Centrale de Lyon, CNRS, Ampère, UMR5005, 69621 Villeurbanne, France, e-mail: romain.delpoux@insa-lyon.fr

Z. Kader · T. Huguet
LAPLACE, Univ Toulouse, CNRS, INPT, UPS, Toulouse, France, e-mail: zohra.kader@laplace.univ-tlse.fr, thomas.huguet@toulouse-inp.fr

magnetic saturations is advantageous. To evaluate the novel observer based flux control, dynamic simulations of SynRM are performed using realistic nonlinear flux characteristics obtained from FEA using FEMM simulation software. The results show that it is possible to efficiently reconstruct the motor flux, flux required for the calculation of the MTPA trajectory of the machine, this, without the use of the notion of differential inductances.

The paper is divided into 4 sections. Section 2 presents motor modelling and the motivations of the article. Section 3 is dedicated to the design of the proposed flux observer. The flux observer allows to propose the flux-control strategy described in Section 4. Finally, the last section, Section 5 is dedicated to the simulation results.

2 Motivations

2.1 SynRM modelling

Figure 1 shows a schematic of the two phases four poles SynRM used in this article. It is a 2 kW machine with maximum torque of 2 N.m.

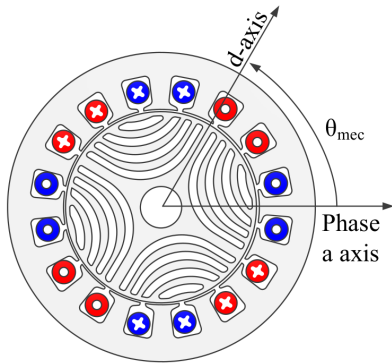


Fig. 1 Schematic of the SynRM.

Two-phase machine (and not a commonly used three-phase) means that voltages are applied to the motor in the two-phase stationary reference frame called $\alpha\beta$. The rotating reference dq -frame is obtained thanks to the Park rotation matrix defined as:

$$(\cdot)_{dq} = P(\theta)(\cdot)_{\alpha\beta}, P(\theta) = \begin{bmatrix} \cos(p\theta) & \sin(p\theta) \\ -\sin(p\theta) & \cos(p\theta) \end{bmatrix}, \quad (1)$$

where $\theta \in \mathbb{R}$ is the rotor mechanical angle and $p \in \mathbb{N}_+$ is the pole pairs number.

The dynamic of the windings in the dq reference frame is given by the state space system:

$$\dot{\lambda}_{dq}(t) = v_{dq}(t) - Ri_{dq}(t) - p\omega(t) \mathcal{J} \lambda_{dq}(t), \quad (2)$$

where $\lambda_{dq}(t) \in \mathbb{R}^2$ is the stator flux linkage, $v_{dq}(t) \in \mathbb{R}^2$ is the stator voltage, $i_{dq}(t) \in \mathbb{R}^2$ is the phase current and $\omega(t) \in \mathbb{R}$ is the rotor angular velocity. The matrix $R \in \mathbb{R}_+$ is the phase resistance diagonal matrix. The matrix \mathcal{J} is a rotation matrix given by $\mathcal{J} = \begin{bmatrix} 0 & -1 \\ 1 & 0 \end{bmatrix}^T$.

The flux-current dependence is a static nonlinear map, where the nonlinearity is introduced by saturation and cross-saturation [14,20]. The apparent inductance is expressed as a nonlinear function $\ell_{dq}: \mathbb{R}^2 \rightarrow \mathbb{R}^2$ yielding to the model:

$$\lambda_{dq} = \ell_{dq}(i_{dq}). \quad (3)$$

The nonlinear function, obtained thanks to FEA using FEMM software are represented Figure 2.

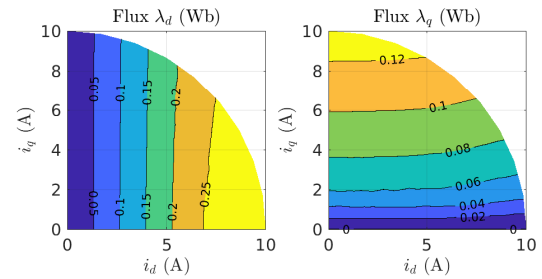


Fig. 2 Nonlinear flux-current characteristic obtained from FEMM.

Assumption 1 Assumes that the nonlinear flux (3) can be approximate by constant inductance supposed to be known and a constant perturbation leading to the linear function:

$$\begin{aligned} \lambda_{dq} &= \ell_{dq}(i_{dq}) = Li_{dq} + \Lambda_{dq}, \\ \dot{\Lambda}_{dq} &= 0, \end{aligned} \quad (4)$$

with $L = \begin{bmatrix} L_d & 0 \\ 0 & L_q \end{bmatrix}$, where $L_d \in \mathbb{R}_+$ and $L_q \in \mathbb{R}_+$ are the autoinductance of the d - and q - axis and $\Lambda \in \mathbb{R}^{2 \times 1}$ is a column vector.

Electric machines produce electromagnetic torque $\tau_{em} \in \mathbb{R}$ when the current interact with the magnetic field, i.e. flux. The torque equation is:

$$\tau_{em} = p i_{dq}^T \mathcal{J} \lambda_{dq}. \quad (5)$$

2.2 Control objective

The control objective is to produce MTPA for the SynRM, while produced tor is depends on the interaction of current

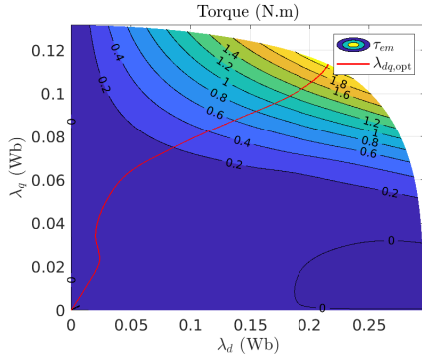


Fig. 3 Torque-flux characteristic and MTPA trajectory (red).

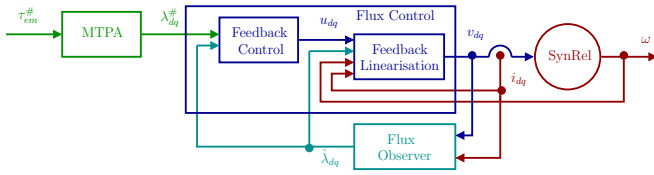


Fig. 4 Representation of the overall observer based flux controller.

and flux which are dependent in a nonlinear manner described equation (3). For a desired torque value, in the feasible domain, MTPA trajectory provides the optimal reference flux $\lambda_{dq}^\#$ to be tracked. Knowing that flux are not measured, an observer is required, insofar as we want to get rid of the classically used LUT, it will allow the reconstruction of these quantities from the measured currents. The MTPA trajectory is computed from Joules losses :

$$P_{\text{Joules}} = Ri_{dq}^T i_{dq}, \quad (6)$$

the criterion therefore consists in minimizing the norm of the current i_{dq} i.e. $\|i_{dq}\|$ which are computed by minimizing the current magnitude. One poses:

$$i_{dq} = I_s \begin{bmatrix} \cos(\gamma) \\ \sin(\gamma) \end{bmatrix}, \quad (7)$$

where I_s is the current magnitude and γ is the current angle [18]. The MTPA trajectory coincides with:

$$\frac{d\tau_{em}}{d\gamma} = 0, \quad (8)$$

which can be computed numerically from the characteristic given Figure 3. The overall torque controller for the SynRM machine is represented on Figure 4.

3 Flux observer

The observer objective is to estimate the flux of the motor while current only is measured. In order to propose this kind of observer, let us consider the dynamical equation (2) with

assumption given equation (4). The system in the augmented states $X^T = [\lambda_{dq}^T \Lambda_{dq}^T]$ can be written as follows:

$$\begin{bmatrix} \dot{\lambda}_{dq} \\ \dot{\Lambda}_{dq} \end{bmatrix} = \begin{bmatrix} -RL^{-1} - p\omega \mathcal{J} & L^{-1} \\ 0 & 0 \end{bmatrix} \begin{bmatrix} \lambda_{dq} \\ \Lambda_{dq} \end{bmatrix} + \begin{bmatrix} I_2 \\ 0_2 \end{bmatrix} v_{dq}, \quad (9)$$

$$= A(\omega)X + Bv_{dq}.$$

Using the relation (4), the output y can be written as

$$y = i_{dq} = [L^{-1} \ -L^{-1}] \begin{bmatrix} \lambda_{dq} \\ \Lambda_{dq} \end{bmatrix} = CX. \quad (10)$$

From the augmented state model, one can compute the observation matrix:

$$O = [C \ CA(\omega) \ CA^2(\omega) \ CA^3(\omega)]^T,$$

one can check that $\text{rank}(O) = 4$ if $\omega \neq 0$, i.e., the system is observable for all $\omega \neq 0$. Thus, using an observer we are able to reconstruct the unmeasured flux variable λ_{dq} as well as the flux uncertainty introduced by the saturation phenomena. In order to do so, we propose the following observer:

$$\begin{aligned} \dot{\hat{\lambda}}_{dq}(t) &= v_{dq} - Ri_{dq} - p\omega \mathcal{J} \hat{\lambda}_{dq} + \gamma(\hat{\lambda}_{dq} - Li_{dq}(t) - \hat{\Lambda}_{dq}), \\ \dot{\hat{\Lambda}}_{dq} &= \beta(\hat{\lambda}_{dq} - Li_{dq} - \hat{\Lambda}_{dq}), \end{aligned} \quad (11)$$

where $\gamma = \begin{bmatrix} \gamma_1 & 0 \\ 0 & \gamma_2 \end{bmatrix}$ and $\beta = \begin{bmatrix} \beta_1 & 0 \\ 0 & \beta_2 \end{bmatrix}$ are the observer gains to be designed in order to ensure that $\hat{\lambda}_{dq}$ and $\hat{\Lambda}_{dq}$ tend to λ_{dq} and Λ_{dq} , respectively, as t tends to infinity. In order to provide constructive method for these gains, let us rewrite (9) as follows:

$$\dot{X} = \mathcal{A}(\omega)X + Bv_{dq} + Ey, \quad (12)$$

where $\mathcal{A}(\omega) = \begin{bmatrix} -p\omega \mathcal{J} & 0_{2 \times 2} \\ 0_{2 \times 2} & 0_{2 \times 2} \end{bmatrix}$ and $E = \begin{bmatrix} -RI_{2 \times 2} \\ 0_{2 \times 2} \end{bmatrix}$. Likewise, the observer is rewritten as

$$\dot{\hat{X}} = \mathcal{A}(\omega)\hat{X} + Bv_{dq} + Ey + GLC(\hat{X} - X). \quad (13)$$

with $G = \begin{bmatrix} \gamma \\ \beta \end{bmatrix}$, L is defined in (4), and C is as in (10).

From the last equations, one can deduce the observation error given by:

$$\dot{e} = \hat{X} - X = (\mathcal{A}(\omega) + GLC)e = \mathcal{A}_o(\omega)e. \quad (14)$$

Now we are able to state the following result.

Proposition 1 Consider system (2) under Assumption 1 (or equivalently system (9), (10)) and the observer (13). If the observer gains are such that $\gamma_1 < 0$, $\gamma_2 < 0$, $\beta_1 < \frac{-(\beta_1 - \gamma_1)^2}{4\gamma_1}$, and $\beta_2 < \frac{-(\beta_2 - \gamma_2)^2}{4\gamma_2}$ then the observation error $\hat{X} - X$ will converge to zero as t tends to infinity.

Proof Consider the observation error dynamic's given by (14). In order to show that $\hat{X} - X$ tends to zero as t tends to infinity, it is sufficient to show that the observation error is asymptotically stable while the gain G satisfies the conditions stated in the proposition. Thus, let us consider the candidate Lyapunov function $V(e) = \frac{1}{2}e^T e$. Its time derivative is given by:

$$\dot{V}(e) = \frac{1}{2}\dot{e}^T e + \frac{1}{2}e^T \dot{e} = \frac{1}{2}e^T (\mathcal{A}_o^T(\omega) + \mathcal{A}_o(\omega))e. \quad (15)$$

Therefore, in order to show the convergence to zero of the observation error it is sufficient to show that

$$\frac{1}{2}e^T (\mathcal{A}_o^T(\omega) + \mathcal{A}_o(\omega))e < 0, \quad (16)$$

$$\text{with } \mathcal{A}_o(\omega) = \mathcal{A}(\omega) + GLC = \begin{bmatrix} \gamma_1 & p\omega & -\gamma_1 & 0 \\ -p\omega & \gamma_2 & 0 & -\gamma_2 \\ \beta_1 & 0 & -\beta_1 & 0 \\ 0 & \beta_2 & 0 & -\beta_2 \end{bmatrix}.$$

The last inequality holds if the matrix $\mathcal{A}_o^T(\omega) + \mathcal{A}_o(\omega)$ is negative definite. This is true if and only if its odd leading principal minors are negative and the even ones are positive. From the definition of $\mathcal{A}_o(\omega)$ and using the fact that ω is measurable, one has:

$$\mathcal{A}_o^T(\omega) + \mathcal{A}_o(\omega) = \begin{bmatrix} 2\gamma_1 & 0 & \beta_1 - \gamma_1 & 0 \\ 0 & 2\gamma_2 & 0 & \beta_2 - \gamma_2 \\ \beta_1 - \gamma_1 & 0 & -2\beta_1 & 0 \\ 0 & \beta_2 - \gamma_2 & 0 & -2\beta_2 \end{bmatrix}.$$

Then, this matrix is negative definite if and only if:

1. $2\gamma_1 < 0$ i.e., $\gamma_1 < 0$ and
2. $\begin{vmatrix} 2\gamma_1 & 0 \\ 0 & 2\gamma_2 \end{vmatrix} = 4\gamma_1\gamma_2 > 0$ which implies that $\gamma_2 < 0$, and
3. $\begin{vmatrix} 2\gamma_1 & 0 & \beta_1 - \gamma_1 \\ 0 & 2\gamma_2 & 0 \\ \beta_1 - \gamma_1 & 0 & -2\beta_1 \end{vmatrix} = 2\gamma_2(-4\gamma_1\beta_1 - (\beta_1 - \gamma_1)^2) < 0$.
Since $\gamma_1 < 0$ and $\gamma_2 < 0$, this inequality is true only if $4\gamma_1\beta_1 + (\beta_1 - \gamma_1)^2 < 0$ i.e if $\beta_1 < \frac{-(\beta_1 - \gamma_1)^2}{4\gamma_1}$
4. finally, we must have $\det \mathcal{A}_o^T(\omega) + \mathcal{A}_o(\omega) = -2\beta_2(2\gamma_2(-4\gamma_1\beta_1 - (\beta_1 - \gamma_1)^2)) - (\beta_2 - \gamma_2)^2(-4\gamma_1\beta_1 - (\beta_1 - \gamma_1)^2) > 0$. Using the three first conditions on γ_1 , β_1 and γ_2 , it comes that the last inequality is satisfied if $-4\beta_2\gamma_2 - (\beta_2 - \gamma_2)^2 > 0$ which is equivalent to $\beta_2 < \frac{-(\beta_2 - \gamma_2)^2}{4\gamma_2}$.

Therefore, when the observer gains satisfy the four conditions above, $\dot{V}(e) < 0$ for all $e \in \mathbb{R}^4$. This ensures that $\lim_{t \rightarrow \infty} e(t) = 0$ which ends the proof.

Remark 1 From the proof of Proposition 1, we can see that if the observer gains respect the cited conditions, the observation error converge asymptotically to zero. Note that, here, and contrarily to the existing results in the literature [18, 19], the observer receives as inputs the voltages, the currents, and the speed of the machine. The LUT are completely removed from the flux observer and control design algorithms.

4 Observer based flux controller

Here, our objective is the regulation of the flux variables with reference flux provided by the MTPA trajectory represented in red on Fig. 3. Note that, in spite of Park transformation, the flux model given equation (2) remains nonlinear. However, having access to the current measurement, speed measurement, and flux reconstruction from the observer developed above, it is possible to apply a feedback linearization control scheme. The proposed control algorithm is thus composed by two parts, a feedback linearization to compensate the nonlinearities and a feedback control to impose the desired closed loop dynamic. Similar approach can be found applied to the current controller of a permanent magnet motor in [5]. Recently, [18, 19] propose a feedback linearization control based on a hybrid observation scheme including flux observers based on LUTs [18, 19]. Here, our objective is to get rid of the use of LUT by replacing them with a flux observer. The proposed control scheme is represented Fig. 4. Note that the reference torque can be directly a torque reference or a reference computed from an outer speed control loop. This outer loop is out of the scope of this article.

4.1 Feedback linearization

Let us choose:

$$v_{dq} = u_{dq} + Ri_{dq} + p\omega \mathcal{J} \hat{\lambda}_{dq}, \quad (17)$$

equation (2) with (17) becomes:

$$\dot{\lambda}_{dq} = u_{dq} + p\omega \mathcal{J} (\hat{\lambda}_{dq} - \lambda_{dq}). \quad (18)$$

Now, by tuning the observer's gains such that the observer dynamic is faster than the desired closed-loop dynamics, equation (18) becomes:

$$\dot{\lambda}_{dq} = u_{dq}. \quad (19)$$

It results in a time invariant linear system, in which the fluxes λ_d and λ_q are independent, leading to pure integrator. This is why this linearization is often called "decoupling".

4.2 Dynamic control

One of the control objectives is to ensure a zero static error, that is why an integral action is added in the feedforward path between the error comparator and the plant. This control strategy generally called type 1 Servo system, since the plant has no integrator [12, p. 743]. The two flux equations being independent, for $k \in \{d, q\}$, one has $\epsilon_k = \int (\lambda_k^\# - \lambda_k) d\tau$, the integrator output and then:

$$\begin{aligned} \dot{\lambda}_k &= u_k, \\ \dot{\epsilon}_k &= \lambda_k^\# - \lambda_k, \end{aligned} \quad (20)$$

with the control:

$$u_k = -k_p \lambda_k - k_I \epsilon_k, \quad (21)$$

with k_p and k_I the control gains to be tuned using Ackerman's formula to impose the dynamics described by a second order system with the classical characteristic polynomial equation $P(s) = s^2 + 2\zeta\omega_n s + \omega_n^2$, where, the parameters ω_n and ζ are the desired closed loop pulsation and damping coefficient.

5 Simulation results

This section illustrates the performance of the proposed approach through simulations where flux nonlinearity is obtained from FEA. As a rough approximation and to highlight the performance of the observer, for the simulation, the autoinductance L given equation (4) is chosen such that $L_d = L_q = 25$ mH. The difference between the approximation and the real nonlinear flux are plotted Fig. 5.

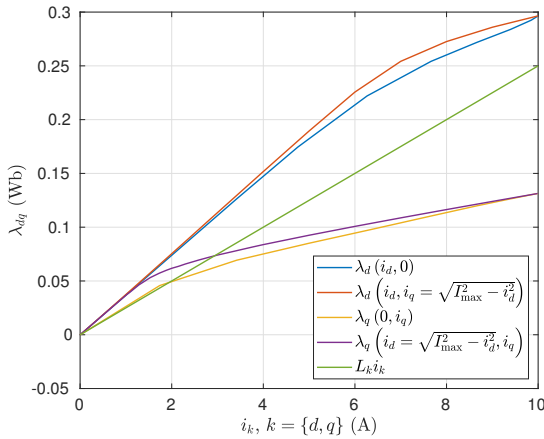


Fig. 5 Representation of the minimal and maximal flux λ_{dq} and autoinductance L_k with respect to current.

For this simulation the torque reference was chosen as a stair sequence with magnitudes equal to [0.2 0.7 1.3 1.8] N.m on a time interval of 2 s. Since the flux is not observable at zero speed, the controller received as input the noted $\lambda_{dq,est}$ defined as:

$$\lambda_{dq,est} = \begin{cases} Li_{dq} & \text{if } t < 2s, \\ \hat{\lambda}_{dq} & \text{else.} \end{cases} \quad (22)$$

The observer gains are set to $\gamma_1 = \gamma_2 = -1$ and $\beta_1 = \beta_2 = 1000$, and the controller gains are chosen to have a closed loop dynamic with 5% overshoot and time response equal to 3 ms leading to the characteristic polynomial with

$\omega_n = 100$ rad/s and $\zeta = 0.7$ and control gain $k_p = 140$ and $k_I = -10000$.

The results for the control strategy are plotted on Fig. 6. It shows that before $t = 2$ s, the flux being wrong, equal Li_{dq} , see equation (22), while the control behaves normally, i.e., controlled to its reference, the desired optimal torque is not reached. This is corrected when the controller receive as input the observed flux after, after $t = 2$ s. The figure then shows that the performance of the observer-based control is good. The observer behavior is plotted on Fig. 7. It is clear that the observed flux converge to the measured one. Moreover, despite Assumption 1, at steps instant, the flux is correctly observed. Finally, the torque-flux characteristic represented on Fig. 8 shows that the MTPA trajectory is not reached at the beginning of the simulation while as soon as the observer is used, the trajectory is correctly tracked.

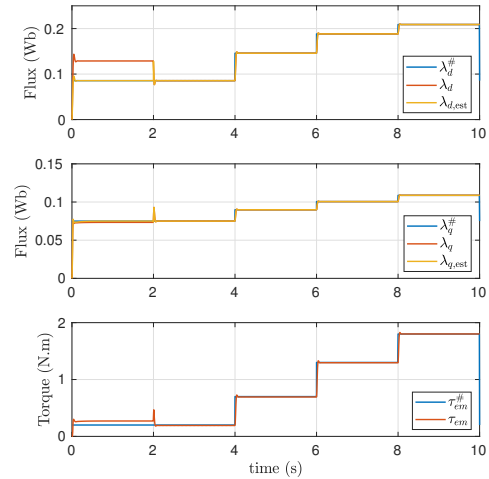


Fig. 6 Chronograph of the simulation results for the control.

6 Conclusion and perspectives

In this paper, was proposed a flux observer of a SynRM motor based on the measurement of the current only despite the presence of saturations and cross-saturations. The observation of the flux makes it possible to synthesis a flux-based control law which, in the presence of saturation, is simpler to implement than classical control. Simulations, with a model obtained from FEA, allow to show the performance of the approach on realistic nonlinearities.

As future work, the stability of the closed loop overall system, observer-controller needs to be proven. Real-world experiments are on the way to evaluate the gap between simulation and experimentation and validate the methodology under real conditions, including the inverter nonlinearities

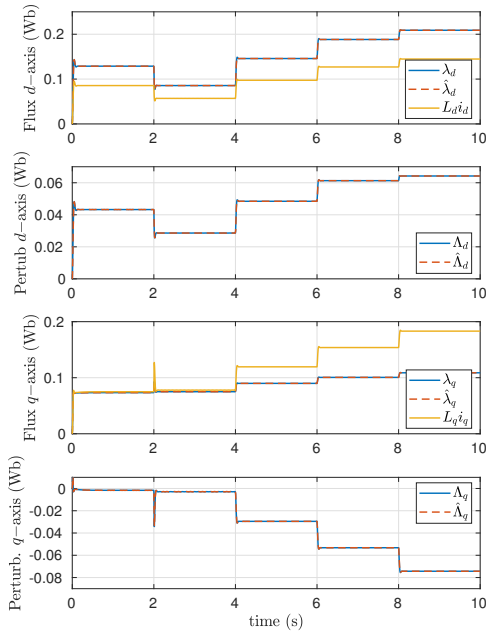


Fig. 7 Chronograph of the simulation results for the observation.

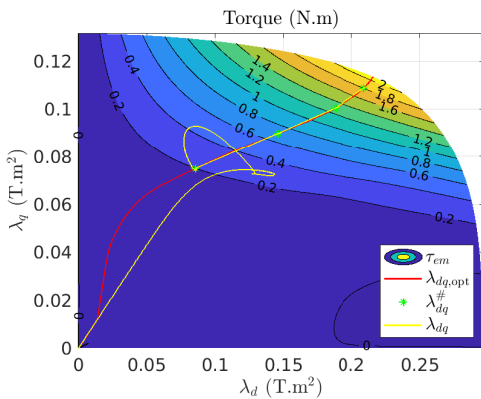


Fig. 8 Torque-flux characteristic, MTPA trajectory, reference and controlled flux.

such as dead-time effect and switching device voltage drop among others. Finally, in this paper, the flux references to provide MTPA trajectory are obtained from the FEA model, an interesting perspective will be the online computation of the MTPA trajectory using on the estimated flux.

References

1. H.-A.-A. Awan, M. Hinkkanen, R. Bojoi, and G. Pellegrino. Stator-flux-oriented control of synchronous motors: A systematic design procedure. *IEEE Transactions on Industry Applications*, 55(5):4811–4820, 2019.
2. B. Ban, S. Stipetić, and M. Klanac. Synchronous reluctance machines: Theory, design and the potential use in traction applications. In *2019 International Conference on Electrical Drives and Power Electronics (EDPE)*, pages 177–188, 2019.
3. Y. Bao, M. Degano, S. Wang, L. Chuan, H. Zhang, Z. Xu, and C. Gerada. A novel concept of ribless synchronous reluctance motor for enhanced torque capability. *IEEE Transactions on Industrial Electronics*, 67:2553–2563, 2020.
4. P. Bernard and L. Praly. Estimation of position and resistance of a sensorless pmsm: A nonlinear luenberger approach for a nonobservable system. *IEEE Transactions on Automatic Control*, 66(2):481–496, 2021.
5. M. Bodson, J.-N. Chiasson, R.-T. Novotnak, and R.-B. Rekowski. High performance nonlinear feedback control of a permanent magnet stepper motor. *IEEE Transactions on Control Systems Technology*, 1:5–14, 1993.
6. A. Boglietti and M. Pastorelli. Induction and synchronous reluctance motors comparison. In *34th Annual Conference of IEEE Industrial Electronics*, pages 2041–2044, 2008.
7. R. Delpoux, T. Huguet, F. Bribiesca Argomedo, L. Queval, J.-Y. Gauthier, and Z. Kader. Finite element dq-model for mtpa flux control of synchronous reluctance motor (synrm). In *2023 IEEE 32nd International Symposium on Industrial Electronics (ISIE)*, pages 1–6, 2023.
8. C. M. Donaghy-Spargo. Synchronous reluctance motor technology : opportunities, challenges and future direction. *Engineering & technology reference.*, pages 1–15, May 2016.
9. H. Kärkkäinen, L. Aarniovuori, M. Niemelä, J. Pyrhönen, and J. Kolehmainen. Technology comparison of induction motor and synchronous reluctance motor. In *IECON 2017-43rd Annual Conference of the IEEE Industrial Electronics Society*, pages 2207–2212, 2017.
10. W. Lee, J. Kim, P. Jang, and K. Nam. On-line mtpa control method for synchronous reluctance motor. *IEEE Transactions on Industry Applications*, 58(1):356–364, 2022.
11. U.S. Department of Energy. Critical materials strategy, 12 2011.
12. K. Ogata. *Modern Control Engineering*. Prentice Hall, 2010.
13. R. Ortega, B. Yi, S. Vukosavić, K. Nam, and J. Choi. A globally exponentially stable position observer for interior permanent magnet synchronous motors. *Automatica*, 125:109424, 2021.
14. M. Preindl and S. Bolognani. Optimal state reference computation with constrained mtpa criterion for pm motor drives. *IEEE Transactions on Power Electronics*, 30(8):4524–4535, 2015.
15. M.-A. Rahman. History of interior permanent magnet motors. *IEEE Industry Applications Magazine*, 19:10–15, 2013.
16. A. Rassolkin, H. Heidari, A. Kallaste, T. Vaimann, J.-P. Acedo, and E. Romero-Cadaval. Efficiency map comparison of induction and synchronous reluctance motors. In *2019 26th International Workshop on Electric Drives: Improvement in Efficiency of Electric Drives*, pages 1–4, 2019.
17. F. Tinazzi, S. Bolognani, S. Calligaro, P. Kumar, R. Petrella, and M. Zigliotto. Classification and review of mtpa algorithms for synchronous reluctance and interior permanent magnet motor drives. In *2019 21st European Conference on Power Electronics and Applications (EPE '19 ECCE Europe)*, pages P.1–P.10, 2019.
18. A. Varatharajan, G. Pellegrino, and E. Armando. Direct flux vector control of synchronous motor drives: A small-signal model for optimal reference generation. *IEEE Transactions on Power Electronics*, 36(9):10526–10535, 2021.
19. A. Varatharajan, G. Pellegrino, and E. Armando. Direct flux vector control of synchronous motor drives: Accurate decoupled control with online adaptive maximum torque per ampere and maximum torque per volt evaluation. *IEEE Transactions on Industrial Electronics*, 69(2):1235–1243, 2022.
20. T.-G. Woo, S.-W. Park, S.-C. Choi, H.-J. Lee, and Y.-D. Yoon. Flux saturation model including cross saturation for synchronous reluctance machines and its identification method at standstill. *IEEE Transactions on Industrial Electronics*, 70(3):2318–2328, 2023.